Effect of the seismic excitation angle on the dynamic response of adjacent buildings during pounding

Panayiotis C. Polycarpou[a], Loizos Papaloizou[b], Petros Komodromos[*]
and Dimos C. Charmpis[c]

*Department of Civil and Environmental Engineering, University of Cyprus, 75 Kallipoleos Str.,
P.O. Box 20537, 1678 Nicosia, Cyprus*

Abstract. The excitation angle or angle of incidence is the angle in which the horizontal seismic components are applied with respect to the principal structural axes during a time history analysis. In this study, numerical simulations and parametric studies are performed for the investigation of the effect of the angle of seismic incidence on the response of adjacent buildings, which may experience structural pounding during strong earthquakes due to insufficient or no separation distance between them. A specially developed software application has been used that implements a simple and efficient methodology, according to which buildings are modelled in three dimensions and potential impacts are simulated using a novel impact model that takes into account the arbitrary location of impacts and the geometry at the point of impact. Two typical multi-storey buildings and a set of earthquake records have been used in the performed analyses. The results of the conducted parametric studies reveal that it is very important to consider the arbitrary direction of the ground motion with respect to the structural axes of the simulated buildings, especially during pounding, since, in many cases, the detrimental effects of pounding become more pronounced for an excitation angle different from the commonly examined 0 or 90 degrees.

Keywords: pounding; incidence angle; bi-directional excitation; adjacent buildings; impact; three-dimensions

1. Introduction

Several research studies have shown that, when performing dynamic analyses of structures, the orientation of the seismic action, i.e., the angle in which the horizontal seismic components are applied with respect to the structural axes, affects significantly the computed response of the simulated structure. In particular, studies have shown that the critical angle of seismic incidence, i.e., the angle in which the structural response exhibits its maximum value, is, in general, different from 0 or 90 degrees with respect to the structural axes of the building, while each response

∗Corresponding author, Ph.D., E-mail: komodromos@ucy.ac.cy
[a]Ph.D., E-mail: ppanikos@ucy.ac.cy
[b]Ph.D., E-mail: loizosp@ucy.ac.cy
[c]Ph.D., E-mail: charmpis@ucy.ac.cy

quantity has its own critical excitation angle (Wilson and Button 1982, Lopez and Torres 1997, Lopez *et al.* 2000, Athanatopoulou 2005, Rigato and Medina 2007, Lagaros 2010a). More specifically, Athanatopoulou (2005) developed analytical formulae for the determination of the critical angle of seismic incidence, as well as the corresponding maximum value, of any response quantity for structures subjected to two or three seismic components and showed, through a practical numerical example, that the critical value for a response quantity can be up to 80% larger than the response produced when the seismic components are applied along the structural axes. Rigato and Medina (2007) examined the influence of the incident angle of the ground motion on several engineering demand parameters in symmetrical and asymmetrical single-storey buildings by performing nonlinear time history analyses considering 39 ground motion pairs. They concluded that peak inelastic deformation demands are underestimated when the horizontal components of ground motion are applied along the principal orientations, while there is not a specific incident angle for which all response parameters attain their maximum value. Lagaros (2010a) performed parametric studies to demonstrate the influence of the incidence angle on the structural response and found that the critical incident angle varies significantly with reference to the intensity level. He also proposed a new procedure for performing multi-component incremental dynamic analysis, which takes into account randomness on both record and incident angle, for the seismic loss estimation in a life-cycle cost assessment procedure (Lagaros 2010b). By performing linear response history analysis of R/C buildings, Kostinakis *et al.* (2012) concluded that the application of the uncorrelated components of the ground motion along the structural axes of a building can lead to significantly underestimated reinforcement with regard to the reinforcement produced for other excitation angles. Torbol and Shinozuka (2012), who investigated the effect of the incidence angle on the fragility curves of bridges, found that, even though the sample bridges were regular and symmetric with respect to the longitudinal axis, the weakest direction is neither longitudinal nor transverse and therefore, if the angle of seismic incidence is not considered, the damageability of a bridge can be underestimated.

It is also widely known that, during strong earthquakes, pounding may occur between buildings that are constructed very close to each other with small or no gap between them, resulting in local light damage or, under certain circumstances, in more severe structural damage. The detrimental effects of pounding of adjacent buildings during strong earthquakes, which have been reported the last few decades (Anagnostopoulos 1995, Kasai and Maison 1997, Cole *et al.* 2012), have motivated many researchers to investigate this phenomenon through numerical simulations and parametric studies, with their majority simulating the problem in two dimensions (2D). The results from the various 2D parametric studies have demonstrated the decisive influence of pounding on the dynamic response of multi-storey buildings and showed the importance of this problem regarding the safety and functionality of these structures. However, the effect of bidirectional horizontal excitation of the buildings, as well as the effect of the incidence angle of the ground motion, cannot be considered when using 2D simulations. Moreover, the limited number of numerical studies that include simulation of the adjacent structures in three dimensions (Papadrakakis *et al.* 1996, Mouzakis and Papadrakakis 2004, Anagnostopoulos and Karamaneas 2008, Jankowski 2009, 2012, Pant and Wijeyewickrema 2012, Efraimiadou *et al.* 2013, Skrekas *et al.* 2014) did not take into account the effect of the direction of the seismic excitation with respect to the structural axes of the buildings. Therefore, a question arises from the combination of the two aforementioned research topics: How does the ground excitation angle with respect to the principal structural axes influence the various effects of pounding between adjacent buildings? Is it important to consider it when performing numerical simulations for the assessment of seismic

pounding in buildings?

In order to provide answers to these questions, extensive investigation that involves numerous dynamic analyses of adjacent multi-storey buildings, considering interactions between them during seismic ground motions, is needed. In relevance to this need, the aim of the current paper is, primarily, to investigate parametrically, through numerical simulations, the effect of the excitation angle on the response of adjacent buildings during pounding and, secondly, to assess the importance of using 3D modelling of structures when investigating such pounding phenomena.

2. Methodology

The numerical simulation of the problem is based on a new, simple and efficient methodology that has been recently published (Polycarpou *et al*. 2014). The basic concepts and assumptions are summarised in the following paragraphs.

2.1 Structural modelling

In the proposed methodology the buildings are modelled as three-dimensional linear elastic multi-degree-of-freedom (MDOF) systems with shear-type behaviour for their storeys in the horizontal direction (Fig. 1). The slab at each floor level of the superstructure is represented by a rigid diaphragm that is mathematically represented by a convex polygon, while the masses are considered to be lumped at the floor levels, having three dynamic degrees of freedom (DOFs), i.e., two translational, parallel to the horizontal global axes, and one rotational along the vertical axis. Therefore, ground excitations only in the horizontal directions are considered, as these are most important for the purposes of the current study; no displacement occurs in the vertical direction, since the translational dynamic DOF of the structure refer only to horizontal planes. Accordingly, it is assumed that the impact forces occur only in horizontal planes. The global stiffness matrix of each building is composed based on the 3×3 stiffness matrices of its storeys, after the latter are assembled by superposing the 3×3 stiffness matrices of all columns of the corresponding storey. For the composition of the global mass matrix of each structure, potential mass eccentricities from the centre of gravity of each floor are considered. Finally, the damping matrix of the building is composed from the stiffness and mass matrices, assuming Rayleigh damping.
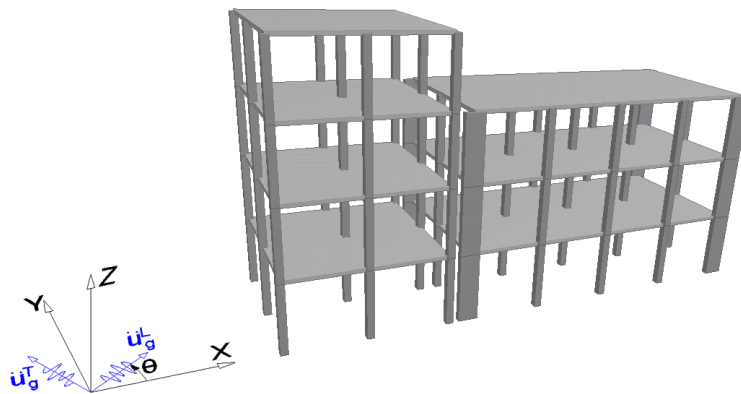

Fig. 1 Three-dimensional modelling of adjacent buildings

The equations of motion of each simulated building can be expressed in matrix form as follows

$$\bar{M} \cdot \underline{\ddot{U}}(t) + \bar{C} \cdot \underline{\dot{U}}(t) + \bar{K} \cdot \underline{U}(t) + \bar{F}_{imp} = -\bar{M} \cdot \left[\bar{I}_L \cdot \ddot{u}_g^L(t) + \bar{I}_T \cdot \ddot{u}_g^T(t) \right] \qquad (1)$$

where $\bar{M}$, $\bar{C}$ and $\bar{K}$ are the mass, damping and stiffness matrices, respectively, $\underline{U}(t)$ is the vector of relative displacements in the global coordinate system at time t, $\bar{F}_{imp}$ is the vector of the computed impact forces, acting on each DOF, while $\bar{I}_L$ and $\bar{I}_T$ are the influence vectors coupling the DOFs of the structure to the two ground motion components $\ddot{u}_g^L(t)$ and $\ddot{u}_g^T(t)$ in the longitudinal and transverse directions, respectively. In particular, the influence vectors for the two horizontal components are provided by the following expressions

$$\bar{I}_L = \begin{bmatrix} \bar{I}_{L,1} & \bar{I}_{L,2} & \dots & \bar{I}_{L,n} \end{bmatrix} \quad \text{and} \quad \bar{I}_T = \begin{bmatrix} \bar{I}_{T,1} & \bar{I}_{T,2} & \dots & \bar{I}_{T,n} \end{bmatrix} \qquad (2)$$

$$\text{where:} \quad \begin{aligned} \bar{I}_{L,i} &= I_X \cdot \cos\theta + I_Y \cdot \sin\theta \\ \bar{I}_{T,i} &= -I_X \cdot \sin\theta + I_Y \cdot \cos\theta \end{aligned} \quad \text{and} \quad \begin{aligned} I_X &= \begin{bmatrix} 1 & 0 & 0 \end{bmatrix}^T \\ I_Y &= \begin{bmatrix} 0 & 1 & 0 \end{bmatrix}^T \end{aligned} \qquad (3)$$

The excitation angle θ is the angle between the principal directions L and T of the excitation orthogonal components, with respect to the global axes of the system X and Y, respectively, as shown in Fig. 1.

The time-history analysis involves the numerical integration of the above differential equations at each time step and the calculation of the resulting displacements, velocities and absolute accelerations at each DOF of each building. Based on the resulting displacements, an automatic check is performed for possible contacts between the floors of the adjacent structures, which would lead to the computation of the arising impact forces to be applied at the corresponding DOFs. The differential equations of all simulated structures are directly integrated simultaneously using the Central Difference Method (CDM), which computes the resulting displacements at time $t+\Delta t$. This characteristic of the method is an advantage in performing the automatic check by the algorithm for the detection of potential impacts between structures at each time-step of the analysis, based on the deformed position of each floor diaphragm in space. For this reason the time-step size, Δt, is selected to be small enough (usually in the range of 1 to 2×10^{-5} sec) to ensure the stability of the numerical method and maximize its accuracy. When an interaction between adjacent structures is detected, the resulting impact forces $\bar{F}_{imp}$ are computed according to the impact model and the methodology that is presented in the next subsection.

2.2 3D Impact model

The majority of the force-based impact models that are available in the literature calculate the impact force as a function of the interpenetration depth between the colliding bodies. This method is widely known as the 'penalty method' in contact mechanics, because an overlapping is allowed between the two bodies in order to calculate the arising impact forces. However, the use of the interpenetration depth as the key variable entails a significant drawback in the case of 3D impact modelling. Specifically, that approach assumes that the calculated impact force depends only on the indentation, regardless of the overall geometry at the contact region. For example, the method assumes that the impact force between two floor slabs, which collide with a specific impact velocity, increases in magnitude in the same way for both cases of side-to-side and corner-to-side impact, which cannot be true.
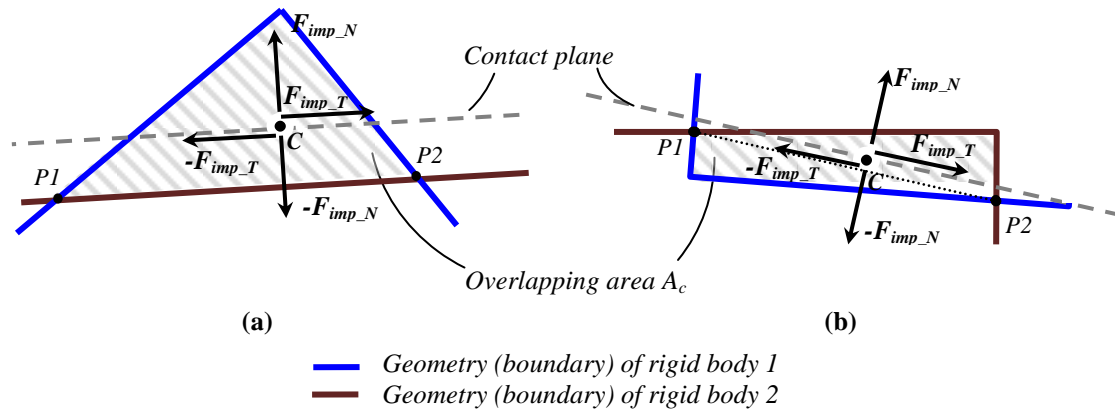
Fig. 2 Schematic representation of the impact model used in the simulations (a) The overlapping region forms a triangle; (b) the overlapping region is a quadrilateral

Therefore, based on the above observation and in order to take into account the geometry at the contact region, the area of the overlapping region, instead of the interpenetration depth, should be used as the key variable in the calculation of the impact forces. Fig. 2 describes schematically how the employed impact model works. In particular, when two slabs, which in the proposed methodology are modelled as polygons, come in contact, they form an overlapping region, which in most of the cases is either a triangle (Fig. 2(a)) or a quadrilateral (Fig. 2(b)). The developed algorithm uses the geometry of the overlapping region at each time-step, defined by the coordinates of its nodes, in order to determine: (i) the location of the action point of the impact forces, (ii) the direction of the impact forces and (iii) the magnitude of the impact forces.

The location of the application point of the impact forces is a very important issue in the case of simulating poundings of buildings in 3D. While in the case of 1D impact models the location of the resultant force vector clearly is at the point of contact, in the case where contact conditions exist over a finite surface area on both bodies, the exact point where the contact force should be applied is not so obvious. For the specific problem of modelling impact between rigid diaphragms, the contact forces in the normal and tangential directions are assumed to act on the centroid C of the overlapping region, and are applied at the corresponding position of the bodies in contact (see Fig. 2).

The normal and tangential directions for the corresponding normal and tangential impact forces are defined using the line that is determined by the two nodes P1 and P2 of the intersection between the boundaries of the two colliding bodies (see Fig. 2). In particular, the normal impact force is perpendicular to this line, which is symbolically called 'contact plane', while the tangential impact force is parallel to it.

An impact stiffness coefficient is used along with the area, A_c, of the overlapping region to calculate the elastic impact force in the normal direction, while the tangential impact force is computed in terms of the relative displacement, $u_{rel,T}$, of the two bodies in contact in the tangential direction. In addition, as in the case of 1D impact models, a viscous impact dashpot is used, in parallel with the impact spring to represent the dissipation of energy during impact (e.g., thermal and acoustic energy) in each impact direction and along with the corresponding relative velocity of the bodies in contact can provide the damping impact force. Therefore, the corresponding total

impact forces in the normal and tangential directions, respectively, taking into account the impact damping, are given by the following expressions

$$F_{imp,N} = F_{imp,N}^{elastic} + F_{imp,N}^{damp} \tag{4}$$

$$F_{imp,T} = F_{imp,T}^{elastic} + F_{imp,T}^{damp} \tag{5}$$

The elastic impact forces in the normal and tangential directions are computed by the following equations, at each iteration time-step

$$^{(t+\Delta t)}F_{imp,N}^{elastic} = {}^{(t)}A_c \cdot k_{imp,N} \tag{6}$$

$$^{(t+\Delta t)}F_{imp,T}^{elastic} = {}^{(t)}F_{imp,T} + {}^{(t)}u_{rel,T} \cdot k_{imp,T} \tag{7}$$

The indices N and T in the above equations indicate the normal and the tangential directions, respectively, as shown in Fig. 2. Accordingly, $k_{imp,N}$ (in kN/m^2) and $k_{imp,T}$ (in kN/m) are the impact stiffness coefficients in the normal and tangential directions, respectively.

Viscous impact damping is assumed to be velocity-proportional and, therefore, the magnitude of the damping force in each impact direction (normal and tangential) is computed using the corresponding relative velocity of the bodies that are in contact, together with an impact damping coefficient

$$^{(t+\Delta t)}F_{imp,N}^{damp} = {}^{(t)}\dot{u}_{rel,N} \cdot c_{imp,N} \tag{8}$$

$$^{(t+\Delta t)}F_{imp,T}^{damp} = {}^{(t)}\dot{u}_{rel,T} \cdot c_{imp,T} \tag{9}$$

where $\dot{u}_{rel,N}$, $\dot{u}_{rel,T}$, $c_{imp,N}$ and $c_{imp,T}$ are the relative velocities and the impact damping coefficients in the normal and tangential directions, respectively. The values of the impact damping coefficients can be approximated in the same manner as in the case of 1D impact models, based on the coefficient of restitution, which can be provided for various materials, and the active masses of the colliding rigid bodies. The corresponding formulas and further details about the estimation of impact parameters (i.e., the impact stiffness and impact damping coefficients) can be found in Polycarpou *et al*. (2014).

In order to take into account friction in the tangential direction of impact, the Coulomb friction law is used to limit the tangential impact force below a certain magnitude that depends on the magnitude of the normal impact force and the static and kinetic friction coefficients of the contact surface

$$\begin{aligned} \text{If } \left| {}^{(t+\Delta t)}F_{imp,T} \right| &\leq \left| {}^{(t+\Delta t)}F_{imp,N} \cdot \mu_s \right| \quad \rightarrow \quad \text{use Equation (5)} \\ \text{If } \left| {}^{(t+\Delta t)}F_{imp,T} \right| &> \left| {}^{(t+\Delta t)}F_{imp,N} \cdot \mu_s \right| \quad \rightarrow \quad {}^{(t+\Delta t)}F_{imp,T} = {}^{(t+\Delta t)}F_{imp,N} \cdot \mu_k \end{aligned} \tag{6}$$

where μ_s and μ_k are the static and kinetic friction coefficients, which are applied in the 'stick' (i.e., no sliding occurs) and 'slide' mode of contact, respectively.

2.3 Developed software

The proposed methodology has been implemented in a software application, specifically developed to effectively and efficiently perform 3D numerical simulations and parametric analyses

of both fixed-supported and seismically isolated buildings, considering pounding. For the development of the software application, modern object-oriented design and programming approaches are utilized, providing the desired flexibility, maintainability and extensibility in order to fulfil the needs of this study, while also facilitating potential extensions to accomplish future research plans. The developed software has a robust Graphical User Interface (GUI) with various capabilities, which has been designed and implemented using the Java Swing API, to facilitate the effective performance of both simulations and parametric analyses. The input data can be either imported from input files or specified using the GUI, while the computed results can be exported in output files or used to generate and store plots and graphical animations in vector formats.

3. Analysis data

Two regular and symmetric reinforced concrete buildings of three and four storeys, respectively, have been selected and used in this study. The typical floor-plans and the side views of the buildings are illustrated in Fig. 3. Although the implemented methodology supports the simulation of more complicated structures with irregularities both in plan and height, the selection of the particular buildings has been made in order to more easily identify the effects of the various parameters on the response during pounding.

All columns sections of the simulated adjacent buildings have dimensions 35×35 cm except from the corner columns of the right 3-storey building C1, C3, C13 and C15, which have dimensions 100×30 cm. The dimensions and arrangement of the columns have been selected in a way to obtain a relatively 'flexible' and a 'stiff' building in the X direction, along which pounding will occur during an earthquake. As is already known, pounding is likely to have more pronounced effects when the adjacent buildings have substantially different dynamic characteristics (Anagnostopoulos and Spiliopoulos 1992, Papadrakakis *et al*. 1996, Jankowski 2008). It is emphasized that the special configurations of the two buildings are specified to facilitate the particular investigation purposes of the present study. Certain design code requirements may impose different column arrangements and/or sizes in practise (e.g., stiffer columns not only along the X direction, but also along the Y direction of the Right building). Due to symmetry, the first two eigenmodes are translational along the two horizontal axes for both structures. The corresponding fundamental periods for the Left building are $T_{X, Left}=T_{Y, Left}=0.471$ sec and for the Right building $T_{X, Right}=0.176$ sec and $T_{Y, Right}=0.365$ sec.

The elastic modulus of concrete has been taken to be equal to 21 *GPa* with a Poisson's ratio equal to 0.2. A uniformly distributed mass of 1000 kg/m^2 has been considered for all floors that resulted to a 64 tons concentrated floor mass for the left building and a 128 tons floor mass for the Right building. A constant viscous damping ratio of 0.05 has been considered for the two extreme eigenfrequencies (first and last eigenmodes) for each of the two buildings in order to compose the corresponding Rayleigh damping matrix. The seismic gap d, i.e., the separation distance between the two buildings, is taken to be 1.0 mm, which corresponds practically to the zero gap case (i.e., the buildings are constructed with no gap between them). The negligible value of d=1 mm was selected instead of the zero value in order to avoid potential numerical errors at the first step of integration. The normal impact stiffness $k_{imp,N}$ is 2.09×10^7 kN/m^2, while the corresponding tangential impact stiffness $k_{imp,T}=4.59 \times 10^6$ kN/m. The impact stiffness values are estimated from the elastic material properties of the colliding adjacent slabs, according to relevant equations (Eqs. (32) and (34)) provided in Polycarpou *et al*. (2014). The static and kinetic friction coefficients are

taken to be μ_s=0.8 and μ_k=0.6, respectively (Tassios and Vintzeleou 1987).

   The seismic records from six major earthquakes of medium to high intensity are used for the performed analyses, including both horizontal seismic components of each ground motion. The main characteristics of the selected seismic records are provided in Table 1, while their corresponding response spectra are provided in Fig. 4, along with the fundamental eigenperiods of the simulated buildings in each horizontal direction. The selection of the particular earthquake excitations was based on the proximity of their predominant frequencies, according to their corresponding response spectra, to the fundamental eigenperiods of the two buildings. No scaling has been applied to the seismic excitation records that have been used.
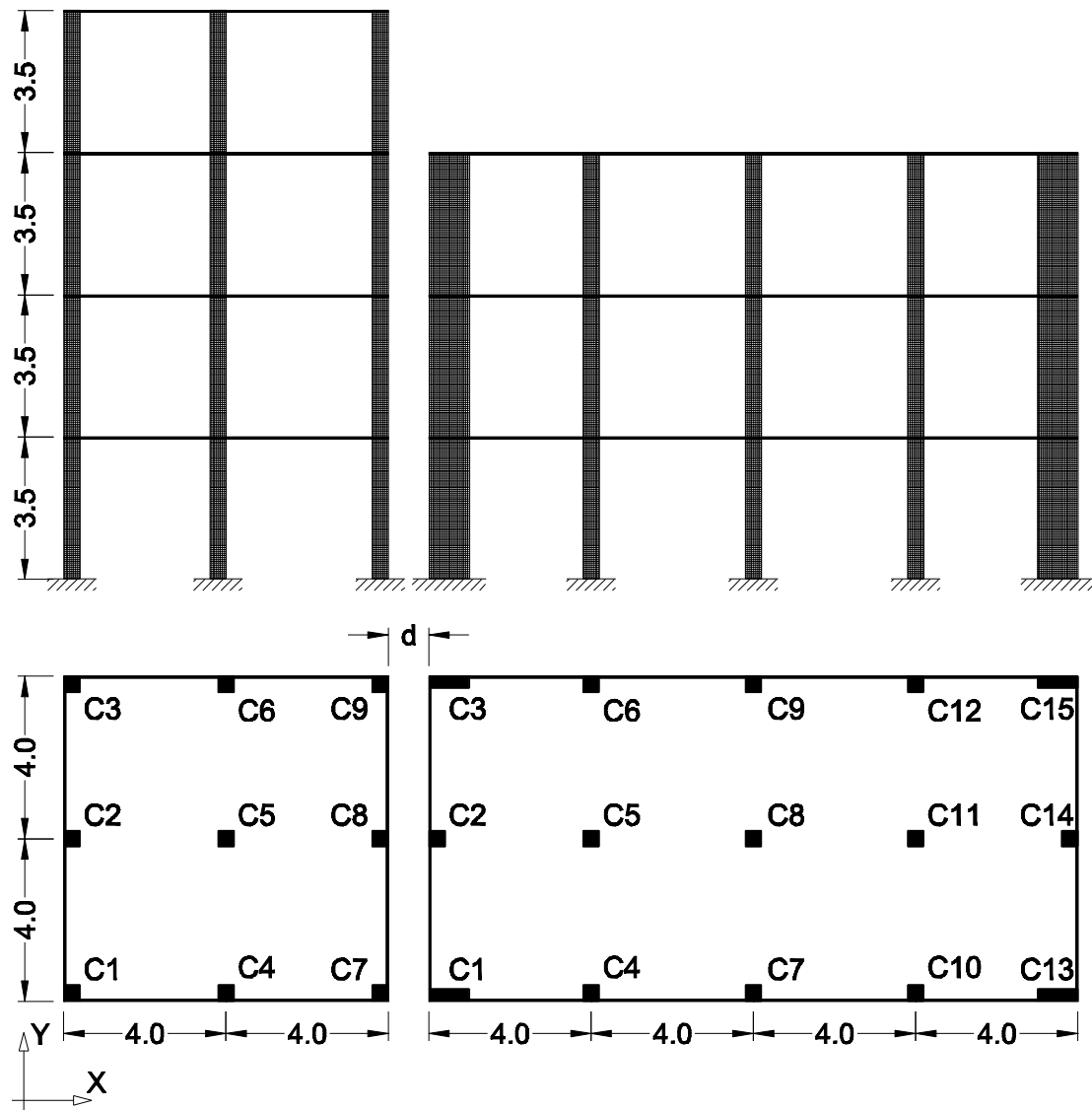

Fig. 3 Side view and plan view of the two simulated adjacent buildings

Table 1 Earthquake records considered in the parametric analyses

Earthquake	Date	Mw	Station	Component	PGA (m/sec^2)
Athens, Greece	07/09/1999	6.0	Kallithea	N46	2.602
				N136	3.013
Thessalonika, Greece	20/06/1978	6.2	City Hotel	E-W	1.431
				N-S	1.365
El Centro, CA, USA	18/05/1940	6.9	Imperial valley irrigation district	S00E	3.417
				S90W	2.10
Kocaeli, Turkey	17/08/1999	7.5	Duzce-Meteoroloji Mudurlugu	SN	3.039
				EW	3.543
Loma Prieta, CA, USA	18/10/1989	6.9	Oakland outer harbor wharf	Ch1-270	2.704
				Ch3-000	2.155
Parkfield, CA, USA	27/06/1966	6.2	Cholame 5W	85	4.257
				355	3.478

Fig. 4 Displacement and acceleration response spectra of (a) the longitudinal and (b) transversal seismic components of the six earthquake records. The fundamental periods of the considered buildings in each direction are also indicated

4. Parametric analyses

In order to investigate the effect of the excitation angle on the structural response during

pounding, large numbers of simulations involving the two adjacent buildings have been performed using the developed software application. Specifically, the two structures have been dynamically analysed simultaneously under each ground motion, with the incidence angle varying from 0 to 180 degrees, with a step of 4 degrees (i.e., 46 simulations for each earthquake). The buildings have been analysed for two different cases; (i) without pounding, i.e., assuming an adequately large clearance between the buildings, and (ii) with pounding, resulting from the lack of any essential clearance (beyond the limited seismic gap of 1.0 mm) between the two buildings. The interstorey deflections are selected as the monitored response quantity, since they can be related with the seismic performance and potential structural damage of a building during an earthquake.

4.1 Results from parametric analysis using the Athens Earthquake

Fig. 5 presents the peak interstorey deflections in the X and Y directions of the corner columns C9 and C3 of the Left and Right building, respectively (see Fig. 3), for the case without pounding and considering the Athens Earthquake as ground excitation. The maximum responses for each storey are plotted in terms of the excitation angle, θ (see Eq. 3). In accordance with previous similar studies, the results reveal that the peak responses depend highly on the incidence angle, especially in the case of the more flexible Left building and the Y direction of the Right building. Specifically, the peak interstorey deflections in the X direction of column C9 range from about 4 mm (storey drift=1.1‰) for the case of θ=150° to 11 mm (storey drift=3.1‰) for the case of θ=50°, resulting to a discrepancy of about 175%. It is also observed that the critical excitation angle (i.e., the angle for which the maximum response occurs) for the deflections in the X direction is nearly common among all floors (about 50°), but is different from the corresponding critical angle for the deflections in Y direction (about 140°), which is also the same for all storeys. Specifically, the difference between the two critical angles is 90 degrees (i.e., complementary angles), since the Left building is symmetrical in both directions.

While in the 'no pounding' case the trends in the plots are smooth (Fig. 5), when pounding occurs the trends become more rough and the behaviour is more complicated, as shown in Fig. 6. Especially in the case of interstorey deflections of column C9 (Left building) in the X direction, which is the direction where impacts occur, the effects of pounding are more pronounced. Specifically, the plots in Fig. 6 show that for a θ between 0 to 90 degrees there is no substantial change in the shape of the trends besides a small increase in the peak responses for all floors. It is observed that for higher values of θ the interstorey deflections at the top storey of the Left building become larger than the ground floor's deflections, which are normally the highest among all floors. That is clearly due to pounding and, more specifically, the excitation of higher modes of deformation of the structure after experiencing impacts. The change in the response is more intense for angles near 90 degrees, probably because the N136 seismic component, which is initially applied in the Y direction, has the largest PGA between the two components. Furthermore, the change in the response-angle relationship due to pounding is not so obvious in the deflections in Y direction, since impacts occur only in the X direction.

In order to make the pounding effects more evident, the peak interstorey deflections during pounding are divided by the corresponding values obtained from the case without pounding, resulting to the so called 'amplification ratio'. The amplifications of the interstorey deflections of columns C9 and C3 of the Left and Right buildings, respectively, are plotted in Fig. 7. It is observed that the top storey's deflections of the taller and more flexible Left building can be amplified up to 3.5 times, depending on the excitation angle. That denotes a substantial increase in
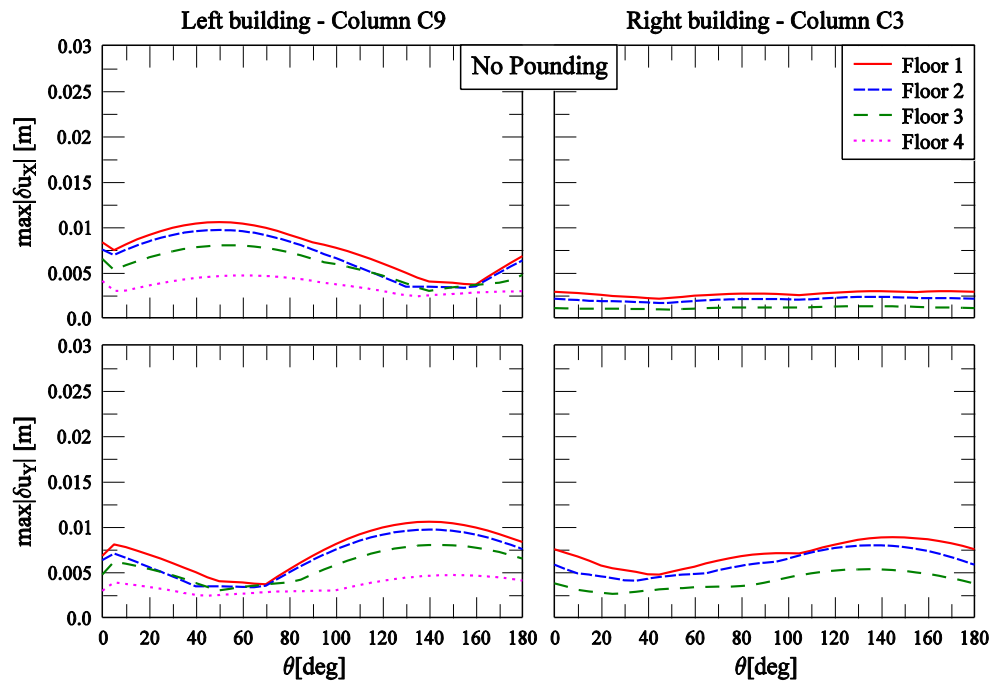
Fig. 5 Peak interstorey deflections of the buildings' corner columns in terms of the excitation angle, considering the 'no pounding' case under the Athens Earthquake
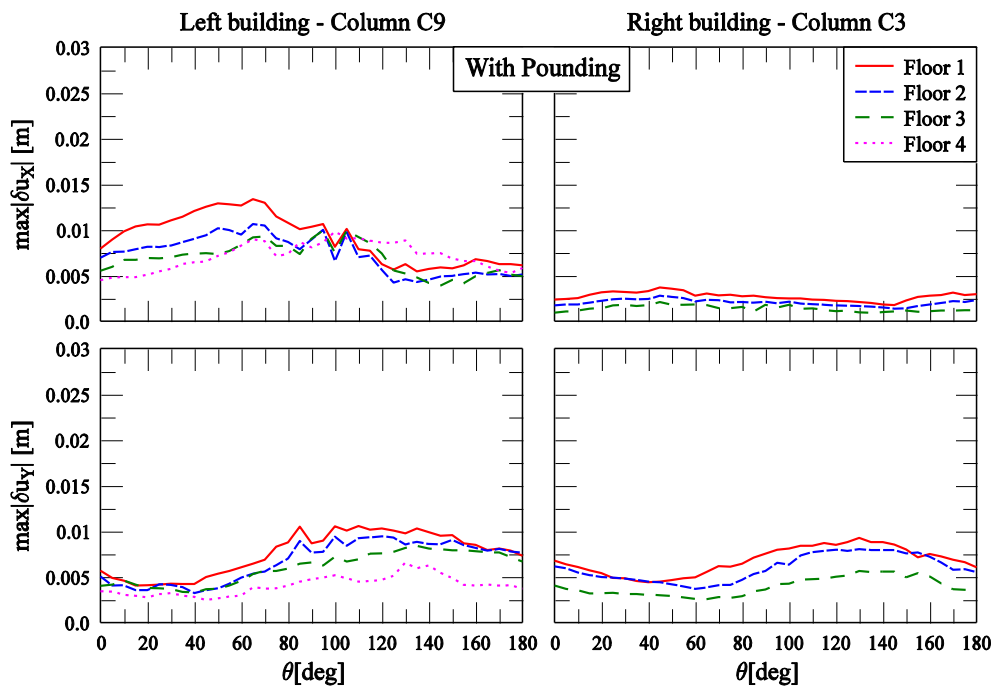

Fig. 6 Peak interstorey deflections of the buildings' corner columns in terms of the excitation angle, considering the case of pounding under the Athens Earthquake
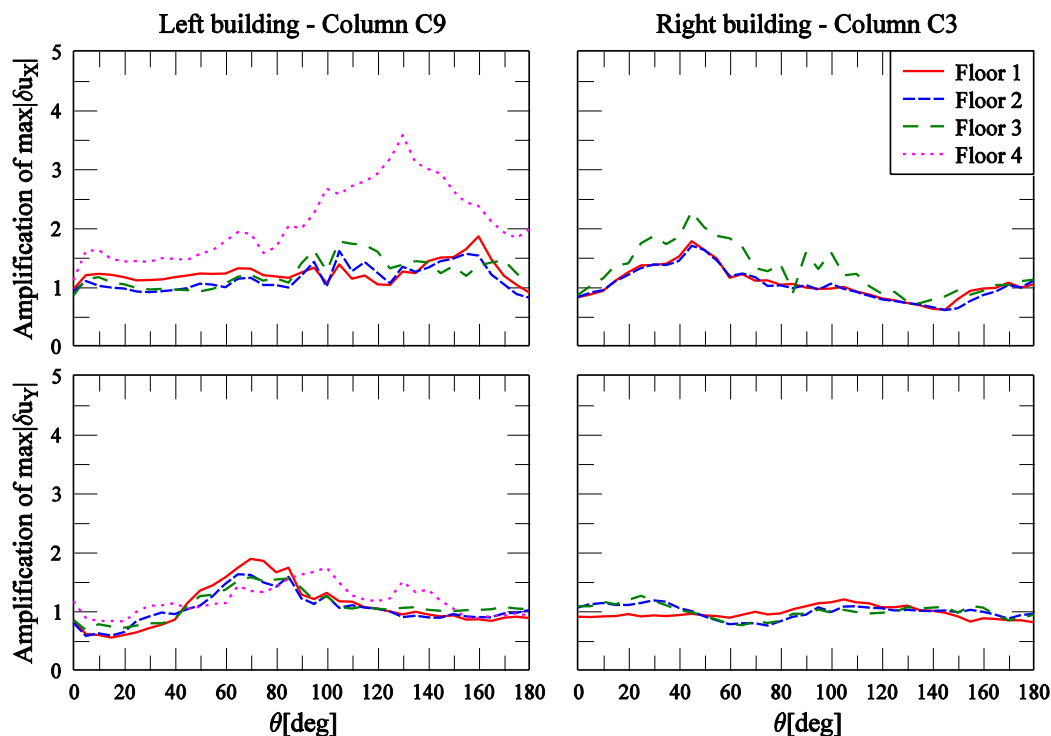
Fig. 7 Amplifications of the peak interstorey deflections due to pounding, in terms of the excitation angle, considering the Athens Earthquake

the ductility demands of the upper storey's columns, not only due to pounding but also due to the arbitrary orientation of the ground excitation with respect to the structural axes of the buildings, which may further increase those demands. Moreover, the angle in which the amplification of the response due to pounding with the adjacent building gets its maximum value is different from the response's critical angle. For example, in the case of the interstorey deflections of column C9 in the X direction at the 4th storey, the angle where the maximum amplification due to pounding occurs is 130°, while the corresponding critical angle is 50° in the case without pounding (Fig. 5) and 65° in the case of pounding (Fig. 6). It is also observed for both buildings that, for most values of the excitation angle θ, the columns deflections at the top storeys (4th story of the Left building and 3rd storey of the Right building) have higher amplification ratios than those at lower storeys, especially in the X direction where impacts occur. Furthermore, it is obvious that it is important to take into account the arbitrary angle of the excitation since for different angles the response can be amplified (amplification ratio>1) or reduced (amplification ratio<1) due to pounding. Finally, Fig. 7 shows that the less affected responses of those examined in the current case are the deflections in the Y direction of the corner column C3 of the Right stiffer building.

4.2 Effect of earthquake characteristics

The same set of simulations has been performed using the six earthquake records listed in Table 1, in order to examine whether the above observations depend on the earthquake

characteristics. The results for the 'no pounding' case are presented in Fig. 8, where the envelopes of the peak interstorey deflections of the two corner columns are plotted for each earthquake in terms of the excitation angle. The computed peak responses indicate that the variation of the response due to the value of the incidence angle depends on the characteristics of the earthquake, in combination with the characteristics of the structure, while the critical excitation angle of a certain response quantity differs among the various earthquakes. Fig. 9 presents the corresponding results for the case of pounding between the two adjacent buildings. It can be seen that there are some variations in shape and form of the trends, while in most of the cases there is an alteration of the critical excitation angle for a response quantity compared with the case without pounding (Fig. 8). For example, in the case of the Parkfield earthquake without pounding, the maximum deflection in the X direction of column C9 of the Left building is about 18.5 mm and the corresponding critical angle is 65°, while after pounding the peak deflection of the same column becomes 25 mm and the critical angle 0°. Nevertheless, the maximum response is not always amplified during poundings. For example in the case of the El Centro Earthquake the X-deflections of column C9 seem to be reduced due to pounding, while the effect of the incidence angle value on the peak response is not as pronounced as in the case without pounding.

This behaviour can be more clearly seen in Fig. 10 where the amplification ratios of the envelopes of peak responses due to pounding (i.e., the ratio of the responses of Fig. 9 over the corresponding responses of Fig. 8) are plotted for each earthquake. Specifically, Fig. 10 shows that, for the El Centro and the Loma Prieta earthquakes and for almost the whole range of the incidence angle values, pounding reduces (amplification ratio<1) the deflections of column C9 in
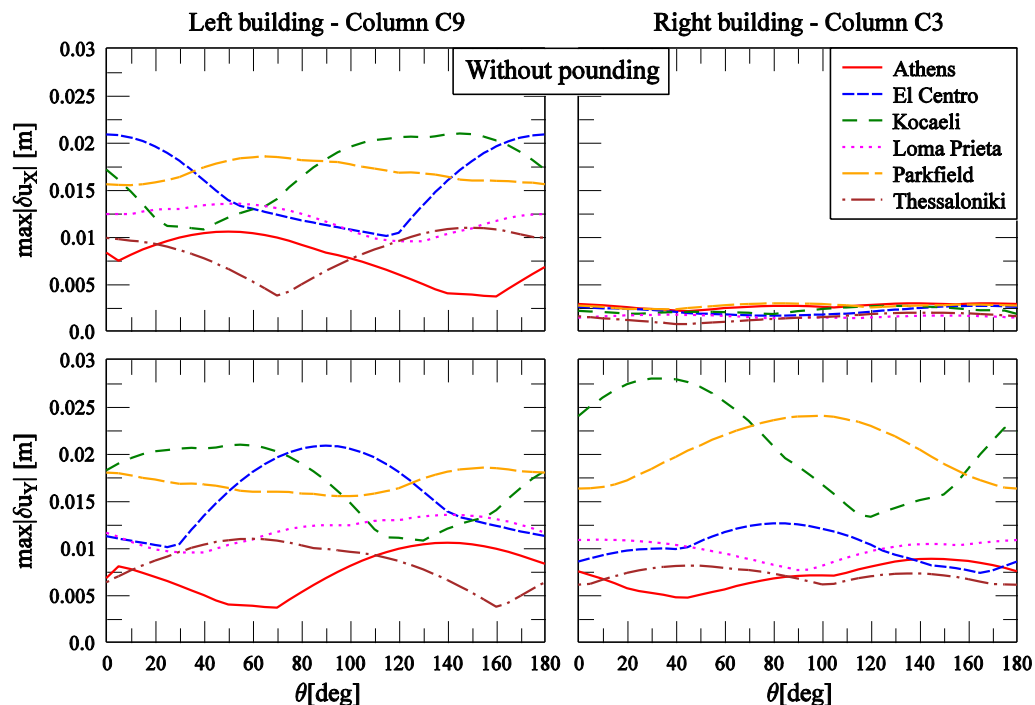

Fig. 8 Envelopes of peak interstorey deflections of the buildings' corner columns in terms of the excitation angle, considering the case without pounding

the *X* direction. Similar reduction of the same response quantity is observed for certain values of the incidence angle of other earthquakes, such as the Parkfield, the Kocaeli and the Thessaloniki earthquakes. However, although in some cases there is a reduction of the response due to pounding for the corner column of the more flexible Left building, the corresponding responses of the column of the stiffer Right building are, in most cases, amplified. This observation complies with similar remarks from previous researchers, who performed numerical simulations using structural models in 2D, where they observed that during seismic pounding between a stiff and a flexible building, the maximum relative displacements of the later were reduced, while the corresponding responses of the stiffer building were amplified (Anagnostopoulos and Spiliopoulos 1992, Mouzakis and Papadrakakis 2004).

It becomes evident from the plots that the angle for which the maximum amplification of the response is observed is not the same for the various earthquakes, while the degree by which pounding affects the response seems to depend on the ground motion characteristics. Finally, it is important to mention that although no pounding occurs in the *Y* direction, the deflections of column C9 in the *Y* direction are also considerably affected from pounding. However, this effect, which also depends on the excitation angle, is not as pronounced as in the case of the same column's deflections in the *X* direction. The most insensitive response quantity to pounding is the column deflection in the *Y* direction of the stiff Right building, for which amplification ratios take rather low values very weakly depending on the variation of the incidence angle.
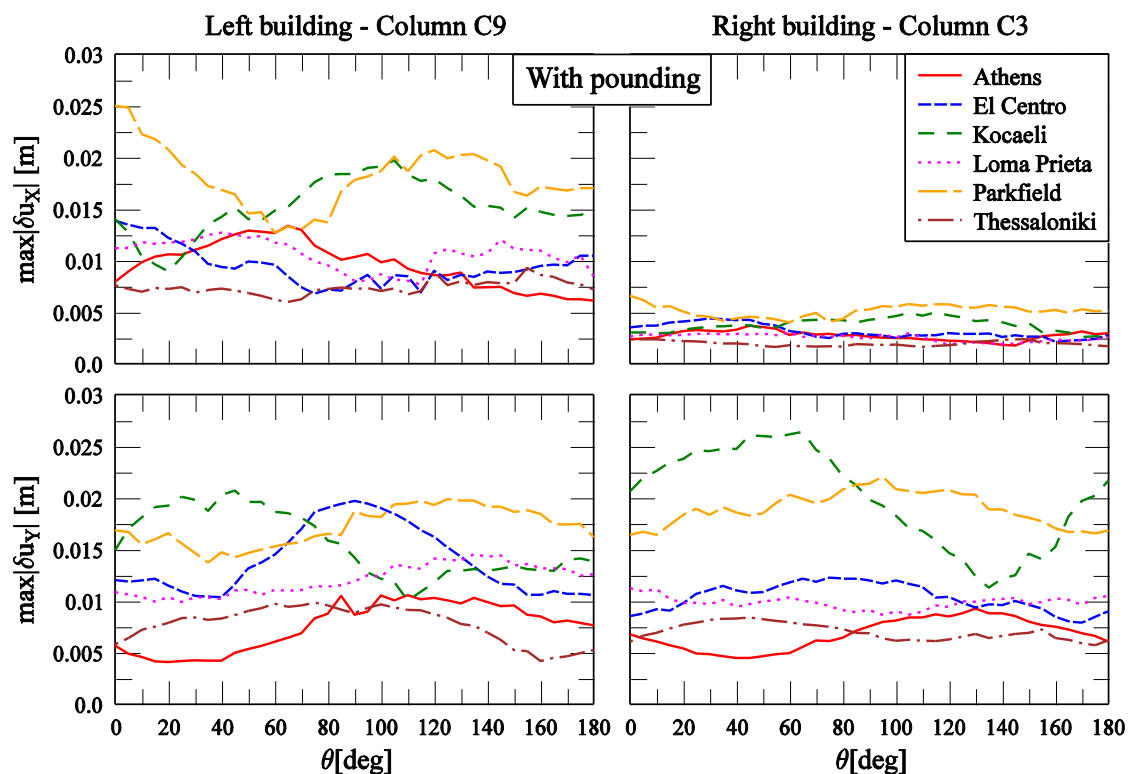

Fig. 9 Envelopes of peak interstorey deflections of the buildings' corner columns in terms of the excitation angle, considering the case of pounding
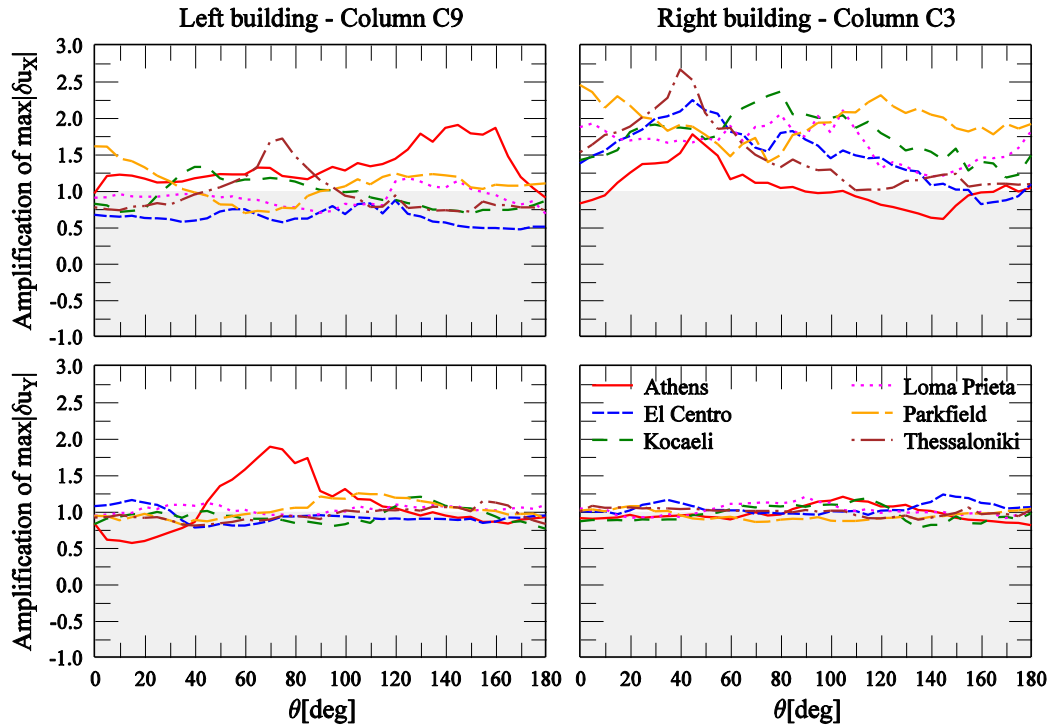
Fig. 10 Amplifications of the envelopes of peak interstorey deflections due to pounding, in terms of the excitation angle

4.3 Effect of accidental mass eccentricity

Many seismic codes demand the consideration of an accidental mass eccentricity when performing dynamic analysis of buildings. For example, Eurocode 8 (2003) suggests an eccentricity of the concentrated floor mass from its nominal location equal to 5% of the floor-dimension perpendicular to the direction of the seismic action. Therefore, it is interesting to examine the effect of the excitation angle on the structural response during pounding in the case of having the floors' masses eccentrically located with respect to the centroids of the corresponding floor slabs. In order to investigate the effect of the mass eccentricity on the response during pounding, a case has been considered where, instead of having the floor masses of the Left building lumped at the centre of gravity of each floor, a mass eccentricity is assumed in both X and Y directions, equal to 40 cm ($e_X=e_Y=0.4$ m), as shown in Fig. 11, which corresponds to 5% of the dimension of the building's side, as suggested by Eurocode 8. In this particular case, no mass eccentricity has been considered for the Right building.

The effect of the excitation angle value has been parametrically studied as described in the previous sections, considering this time the new structural properties of the Left building and the Athens Earthquake records as the ground motion. The plots in Fig. 12 present the amplification of the interstorey deflections of the corner columns of the two buildings. Note that for calculating the amplifications of the Left building the response during pounding has been divided by the corresponding response without pounding, but taking into account the mass eccentricities.
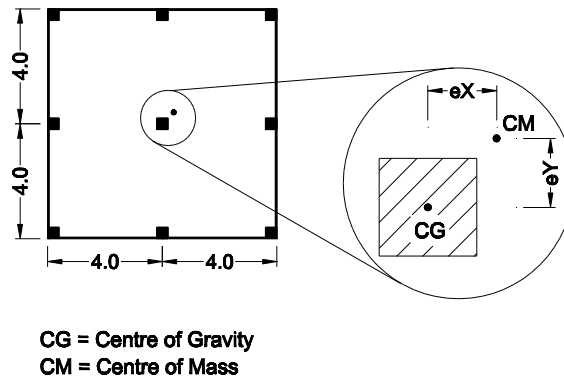
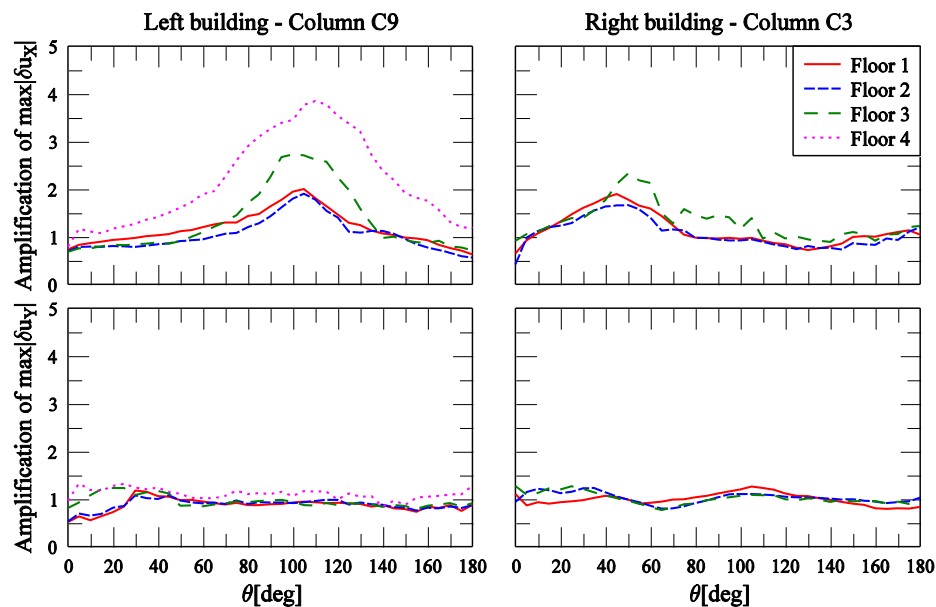Fig. 11 Definition of accidental floor mass eccentricity for the Left building

Fig. 12 Amplifications of the peak interstorey deflections due to pounding, in terms of the excitation angle, considering the Athens Earthquake and an accidental floor mass eccentricity of 5% for the Left building

Comparing the plots with those in Fig. 7 (without mass eccentricities), it can be observed that there is a minor change in the amplifications of the Left building due to pounding, after applying the floor mass eccentricities, while the response of the Right building seems to be unaffected by the mass eccentricities of the Left building, since the trends remain almost the same. More specifically, in the case of the more flexible Left building, the eccentricities of the floor masses seem to slightly increase the effects of pounding since, for most incidence angles, the amplifications of the interstorey deflections in the *X* direction become higher than in the case without eccentricities (Fig. 7). This increase of the pounding effects due to the eccentricities is more pronounced for the lower storeys and occurs in a range of excitation angle values between
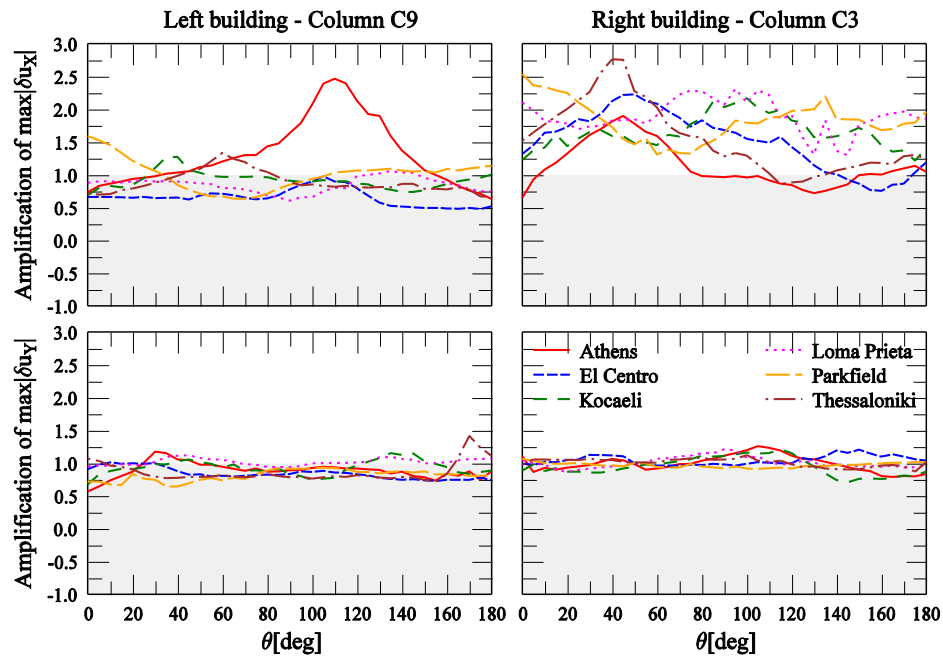
Fig. 13 Amplifications of the peak interstorey deflections due to pounding, in terms of the excitation angle, considering all six earthquakes and an accidental floor mass eccentricity of 5% for the Left building

$80\text{-}140^{o}$, with the peak at 110°, in contrast to the case without eccentricities where the critical angle for amplifications was 130°. It is interesting here to observe that, for an excitation angle equal to 110°, the deflections in the *X* direction of column C9 are amplified from 2 to 4 times, while, for the case of 0°, which is the most typical case (with the seismic components applied along the structural axes), there is no amplification of the response due to pounding. This means that, for the case of an excitation angle of 110°, the ductility demands for the columns of the Left building will increase up to 4 times during pounding compared to the case of an incidence angle of 0°, which is most commonly applied in standard structural analysis and design procedures.

Fig. 13 demonstrates the effect of mass eccentricities by plotting the amplifications of the envelopes of the maximum interstorey deflections, considering all six earthquakes. When comparing these plots with those in Fig. 10, which represent the case without eccentricities, it is observed that, in contrast to the case of the Athens Earthquake, the mass eccentricities do not significantly affect the amplification of the peak interstorey deflections. Specifically, the amplifications of column deflections of both buildings remain nearly the same as in the case without eccentricities, except of those for the case of the Athens earthquake. Thus, it seems that the ground motion characteristics may play some role in the degree by which the eccentricities affect the structural response.

5. Conclusions

The effects of the seismic excitation angle on the response of two adjacent buildings during

pounding have been parametrically examined using a specially developed software application that implements a simple and efficient methodology for simulating multi-storey buildings in three dimensions. The methodology involves the usage of a novel 3D impact model that takes into account the arbitrary location of impact points, as well as the random geometry at the vicinity of impact, when calculating the magnitude and the direction of the impact forces.

The results of the parametric studies reveal that it is very important to consider the arbitrary direction of the ground motion with respect to the structural axes of the simulated buildings, especially during pounding.

Specifically, according to the obtained results:

The detrimental effects of pounding may become more severe for certain values of the excitation angle, different from 0 degrees, which is the most commonly applied in practice when performing time history analysis. For the cases examined, the ductility demands, in terms of interstorey deflections, can be amplified up to 4 times in some cases due to pounding for certain excitation angles different from 0 or 90 degrees, compared to the case of having an incidence angle of 0 degrees, where no response amplification occurs due to pounding.

The incidence angle, in which the amplification of the response due to pounding with the adjacent building gets its maximum value, generally differs from the corresponding critical incidence angle for the same response without pounding.

The effect of the incidence angle on the amplifications of columns' deflections during pounding is influenced by the characteristics of the ground motion in combination with the structural properties.

The most sensitive responses to the variation of the excitation angle, as well as to the mass eccentricity effects, are the interstorey deflections in the direction of pounding and especially those of the more flexible and taller building.

The highest amplifications of the response due to pounding occur at the upper floors of the colliding buildings. Nevertheless, there are cases where, for a range of excitation angle values, the interstorey deflections in the direction of impacts are reduced due to pounding, especially those at lower floors.

In general, the degree by which the incidence angle affects the amplifications of columns deflections doesn't seem to be significantly affected by the mass eccentricities. However, this appears to depend on the ground motion characteristics, since for one of the six earthquakes the consideration of an accidental mass eccentricity of 5% resulted in more pronounced effects of pounding on the response of the taller and more flexible building.

Furthermore, the current study demonstrates the importance of performing three-dimensional time-history analysis when investigating the effects of seismic pounding on the response of adjacent structures. Specifically, the use of 3D dynamic analysis can reveal the effects of certain factors that are directly related to the spatial movement of the buildings, such as the bi-directional excitation and the angle of incidence, on the response during pounding. Since the computational demands are often large when performing 3D dynamic analyses involving impact phenomena, especially in the case of conducting parametric studies, it is crucial to implement an efficient methodology with simple structural and impact modelling, as the one used in the present study.

Acknowledgements

References

Anagnostopoulos, S.A. (1995), "Earthquake induced poundings: State of the art", *Proceeding of the 10th European Conference on Earthquake Engineering*, Duma, Ed. Balkema, Rotterdam.

Anagnostopoulos, S.A. and Karamaneas, C.E. (2008), "Use of collision shear walls to minimize seismic separation and to protect adjacent buildings from collapse due to earthquake-induced pounding", *Earthq. Eng. Struct. Dyn.*, **37**(12), 1371-1388.

Anagnostopoulos, S.A. and Spiliopoulos, K.V. (1992), "An investigation of earthquake induced pounding between adjacent buildings", *Earthq. Eng. Struct. Dyn.*, **21**(4), 289-302.

Athanatopoulou, A.M. (2005), "Critical orientation of three correlated seismic components", *Eng. Struct.*, **27**(2), 301-312.

Cole, G.L., Dhakal, R.P. and Turner, F.M. (2012), "Building pounding damage observed in the 2011 Christchurch earthquake", *Earthq. Eng. Struct. Dyn.*, **41**(5), 893-913.

Efraimiadou, S., Hatzigeorgiou, G.D. and Beskos, D.E. (2013), "Structural pounding between adjacent buildings subjected to strong ground motions. Part I: the effect of different structures arrangement", *Earthq. Eng. Struct. Dyn.*, **42**(10), 1509-1528.

Eurocode 8 (2004), "Design of structures for earthquake resistance - Part 1: General rules, seismic actions and rules for buildings", EN 1998-1:2004.

Jankowski, R. (2008), "Earthquake-induced pounding between equal height buildings with substantially different dynamic properties", *Eng. Struct.*, **30**(10), 2818-2829.

Jankowski, R. (2009), "Non-linear FEM analysis of earthquake-induced pounding between the main building and the stairway tower of the Olive View Hospital", *Eng. Struct.*, **31**(8), 1851-1864.

Jankowski, R. (2012), "Non-linear FEM analysis of pounding-involved response of buildings under nonuniform earthquake excitation", *Eng. Struct.*, 37, 99-105.

Kasai, K. and Maison, B.F. (1997), "Building pounding damage during the 1989 Loma Prieta earthquake", *Eng. Struct.*, **19**(3), 195-207.

Kostinakis, K.G., Athanatopoulou, A.M. and Avramidis, I.E. (2012), "Orientation effects of horizontal seismic components on longitudinal reinforcement in R/C frame elements", *Natl. Hazards Earth Syst. Sci.*, **12**(1), 1-10.

Lagaros, N.D. (2010a), "Multicomponent incremental dynamic analysis considering variable incident angle", *Struct. Infrastr. Eng.*, **6**(1-2), 77-94.

Lagaros, N.D. (2010b), "The impact of the earthquake incident angle on the seismic loss estimation", *Eng. Struct.*, **32**(6), 1577-1589.

Lopez, O.A. and Torres, R. (1997), "The critical angle of seismic incidence and the maximum structural response", *Earthq. Eng. Struct. Dyn.*, **26**(9), 881-894.

Lopez, O.A., Chopra, A.K. and Hernandez, J.J. (2000), "Critical response of structures to multicomponent earthquake excitation", *Earthq. Eng. Struct. Dyn.*, **29**(12), 1759-1778.

Mouzakis, H. and Papadrakakis, M. (2004), "Three dimensional nonlinear building pounding with friction during earthquakes", *J. Earthq. Eng.*, **8**(1), 107-132.

Pant, D.R. and Wijeyewickrema, A.C. (2012), "Structural performance of a base-isolated reinforced concrete building subjected to seismic pounding", *Earthq. Eng. Struct. Dyn.*, **41**(12), 1709-1716.

Papadrakakis, M., Apostolopoulou, C., Zacharopoulos, A. and Bitzarakis, S. (1996), "Three-dimensional simulation of structural pounding during earthquakes", *Eng. Mech.*, **122**(5), 423-431.

Polycarpou, P.C., Papaloizou, L. and Komodromos, P. (2014), "An efficient methodology for simulating earthquake-induced 3D pounding of buildings", *Earthq. Eng. Struct. Dyn.*, **43**(7), 985-1003.

Rigato, A.B. and Medina, R.A. (2007), "Influence of angle of incidence on seismic demands for inelastic single-storey structures subjected to bi-directional ground motions", *Eng. Struct*., **29**(10), 2593-2601.

Skrekas, P., Sextos, A. and Giaralis, A. (2014), "Influence of bi-directional seismic pounding on the inelastic demand distribution of three adjacent multi-storey R/C buildings", *Earthq. Struct.*, **6**(1), 71-87.

Tassios, T.P. and Vintzeleou, E.N. (1987), "Concrete-to-concrete friction", *J. Struct. Eng.*, **113**(4), 832-849.

Torbol, M. and Shinozuka, M. (2012), "Effect of the angle of seismic incidence on the fragility curves of bridges", *Earthq. Eng. Struct. Dyn*., **41**(14), 2111-2124.

Wilson, E.L. and Button, M.R. (1982), "Three-dimensional dynamic analysis for multi-component earthquake spectra", *Earthq. Eng. Struct. Dyn*., **10**(3), 471-476.

SA